GENERAL LECTURE:

THE ROOF WING OPENING SYSTEM OF THE UAE PAVILION AT EXPO 2020

Paolo Leutenegger [1,2]*, Carlo Vergano [1,2], Rainer Herzinger [3], Jürgen Weber [4], Nicola Bassetto[1], Fabio Belluschi[1], Riccardo Cardani[1], Ina Costin[1], Costanzo Codari[1], Stefano Ferla[1], Giovanni Forti[1], Simon Köhler[4], Roberto Maddalon[1], Gino Pari[2], Daniel Panev[2], Michele Pavanetto[1], Cristian Poli[1], Massimo Ripamonti[1], Alessandro Rossignoli[1], Matteo Traù[2], Jonas Uhlmann[4], Renzo Zaltieri[1]

[1]*Duplomatic Motion Solutions S.p.A., Via Mario Re Depaolini 24, 20015 Parabiago (MI), Italy*

[2]*Duplomatic Middle East LLC, Office 3 Rooftop, MSM 2 Bldg. Al Safa 1st, Sheikh Zayed Rd - Dubai*

[3]*Santiago Calatrava LLC, Parkring 11, CH-8002 Zürich, Switzerland*

[4]*Technical University Dresden, Chair of Fluid-Mechatronic Systems, Helmholtzstr. 7a, 01069 Dresden, Germany*

* Corresponding author: Tel.: +39 329 1010322; E-mail address: p.leutenegger@duplomatic.com

ABSTRACT

The UAE Pavilion will be a major attraction at Expo 2020 in Dubai. The roof of the building consists of 28 operable wings made of carbon and glass fiber, having masses ranging from 5 to 18 tons and total lengths in the range of 30 to 65 m that have to be actuated by a dedicated mechanism.

In this paper we present the turn-key project for the design, manufacturing, installation, test and commissioning of the Roof Wing Opening System, which represents a unique system world-wide for operating the wings. It consists of one Hydraulic Power Unit with approximately 1 MW of installed power, 2 km of piping working at the nominal pressure of 210 bar, 46 hydraulic cylinders with 1.5 tons of mass each and the complete automation and control subsystem that includes 9 separate PLCs, dedicated software, 2.000 sensors and control points, and over 20 km of harness.

One major challenge is the control of the wings. Part of them, due to their huge dimensions and masses, are actuated using two or three hydraulic cylinders that have to be properly synchronized during the movement, preventing unwanted displacements in order to avoid stresses on the wing mechanical structure and ultimately permanent damages. Due to the nature of the project, a final validation of the control algorithms can be done only at system level during the commissioning phase. Therefore, particular care has to be devoted to the verification strategy, anticipating the behavior of the system in the early validation stages and following a V-model approach, in order to identify critical situations and reduce the overall risk.

After a brief system description, we will explain how the verification has been approached by using system level simulations and dedicated testing activities on specific subsystems. In particular, we will detail the verification of the control algorithms that has been performed on a dedicated Hardware-In-the-Loop system first, followed then by dedicated tests on a reduced wing mock-up, allowing the study of the system behavior under the most critical conditions. These include the application of external forces with specified profiles. Finally, we will provide the actual status of the system installation, testing and commissioning activities that have been running in Dubai since January 2019.

Keywords: Hydraulic System, Piping, Valves, Hydraulic Actuators, Motion Control, Synchronization

1. THE UAE PAVILION AT EXPO 2020

The UAE Pavilion at Expo 2020 is designed by the Architect Santiago Calatrava in the shape of a falcon in flight, the official symbol of the UAE, and will be a major attraction at Expo 2020. The roof of the building consists of 28 carbon and glass-fiber shaped movable wings, having masses ranging from 5 to 18 tons and total lengths in the range of 30 to 65 m. They are actuated by a hydraulic system called Roof Wing Opening System (RWOS) that is going to be discussed in the following paragraphs.

This special application generated a quite unusual list of requirements to be compliant with, a step ahead of the common requests typical of industrial applications. Since the beginning of the project, we became aware that it was mandatory to have a different approach and an open mindset to provide a technical solution fulfilling the requirements that are beyond usual expectations.

Functionality and good performance were not

Figure 1: Pictorial view of the UAE Pavilion at Expo 2020, Dubai.

enough, the final aim of the project was to realize something to let people astonish, a glimpse of perfection which is the expected target for this event and a special town like Dubai. The final Customer was not just looking for something simply working, but to be delighted with. This awareness accompanied us throughout the development of the whole project.

Our purpose has been at highest level to provide a system giving the impression of absolute precision and solemnity during the movement, being compliant with the environment, the Expo 2020 sustainability idea and the expectations of the Client in terms of performance, reliability and aesthetics. Translating it into requirements it means: All wings shall be opened and closed in a synchronized harmonic simultaneous fashion, absolutely silently, with the lowest possible visual impact, having the highest reliability, high power efficiency, implementing a technical solution devoted to solidity and stability.

Based on the above a technical solution was developed from a reference design and a set of performance specifications. The design development was supported by continuous collaborations with the CI Team, giving us the possibility to develop and optimize the system architecture.

The hydraulic system structure has been defined trading-off the system characteristics, the limited available space inside the building and the aggressive time schedule of the construction. All equipment, including the piping network have been prefabricated in Europe and delivered to Site for installation. As an example, the detailed design allowed the installation of approx. 1,3 km of system piping fully prefabricated without realizing any welding on site.

2. THE ROOF WING OPENING SYSTEM

2.1. Hydraulic Concept

The hydraulic system architecture includes:

- One Hydraulic Power Unit (HPU) with approx. 1 MW of capacity located in the basement of building.
- One piping network implementing the hydraulic backbone of the system. The piping system is composed by two lines: Pressure supply line and Return line. Both start from the HPU and connect to the roof area.
- 46 Valve Stands to independently control the movement of each hydraulic actuator including pressure sensors.
- 46 Hydraulic Actuators equipped with stroke and proximity sensors.
- One Automation and Control Subsystem (AUT) that includes 17 electronic cabinets and more than 20 km of cables.

The basic design idea is to control flow rate and system pressure independently, adjusting them

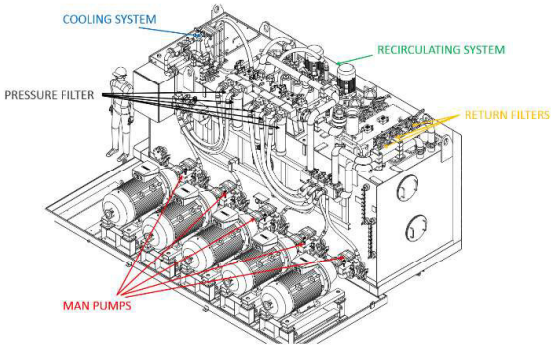

Figure 2: RWOS Hydraulic Power Unit.

according to every specific working condition. For this reason, fixed displacement pumps controlled by electrical motors driven by inverters have been used. This allows an almost instantaneous setting of the system pressure according to the specific load request.

The max oil flow rate has been calculated based on the time requirements specified for wing opening and fast closing sequences. Flow rates have been calculated individually for every actuator taking into consideration their cinematic characteristics and acceleration and deceleration profiles. Since the main architectural project requirement considers the synchronous opening and closing of all wings simultaneously, they have been finally combined in order to obtain the total flow rate required by the working cycle, as shown by the blue curve of **Figure 3**, where the worst-case opening cycle is considered.

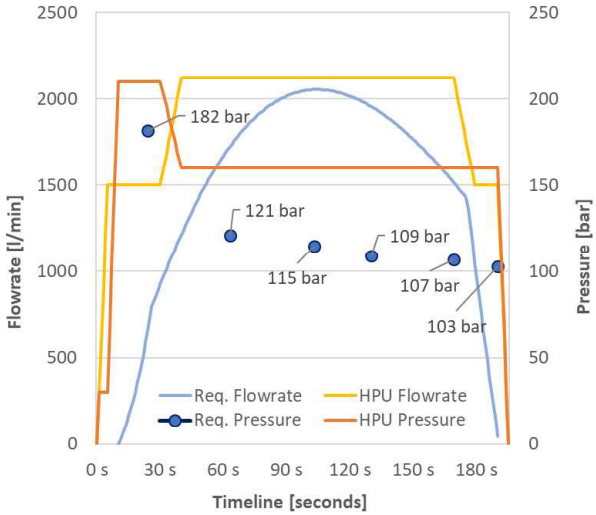

Figure 3: System level requirements and HPU parameters for the opening cycle (180 seconds) under worst-case load conditions.

The system design pressure has been defined in accordance to the dynamic load requirements calculated for every actuator. The envelope of the pressure required for the movement for given angular positions of the wing has been calculated considering the worst-case load condition having both the effect of gravity and the load generated by the wind. Relevant wind load data have been derived from a dedicated test campaign with a representative UAE Pavilion model in the wind tunnel, in which a complete pavilion model including all surrounding buildings has been used to measure wing loads using approximately 900 pressure sensors.

The resulting pressure requirement for allowing the movement of the system is shown by the blue dots in **Figure 3**.

In order to minimize the power consumption, flow rate and system pressure are regulated according to the working cycle. Due to the cinematic law, the acceleration and deceleration phases and the dependence of the loads from the wing angular position, the pressure request is maximum at the beginning of the opening movement, where the flow rate request is at minimum. After acceleration, the pressure request decreases while flow rate demand increases. This defines a trade-off between pressure and flow rate, giving the possibility to optimize the power consumption.

The HPU generated flow rate and output pressure applied on the P-line are shown by the orange and yellow curves respectively.

The request of having a silent movement drives the choice to use internal gear pump, to introduce bumper elements on all piping system and to define the start-up sequence in order to minimize the possibility of vibration.

Among high-pressure pumps, internal gear pumps are in fact those with lowest noise emission. Additionally, two pumps on each pump unit have been foreseen. Twin pumps have been installed in such a way to have pulsation in counter-phase, thus reducing pressure ripple on the pressure line and consequently the noise emission.

2.2. System Piping

System Piping has been designed taking into consideration different constrains. The main requirement is to guarantee high-pressure hydraulic fluid flowrate at big distance from the HPU (Hydraulic Power Unit), where pressure is generated. This has to be achieved considering the structure deformation of the building, desertic climate that includes extreme temperature excursions, sand storms and heavy rains, different elevations of actuators and power generation.

Non-painted stainless steel 316L has been selected as piping material. This is considered as the most reliable measure to guarantee functionality throughout the pavilion's lifetime, limiting the maintenance demand.

The HPU is designed in order to provide a maximum constant 210bar working pressure with more than 2000l/min flow rate. A schematic picture showing the location of the HPU and the routing of the system piping inside the Pavilion is shown in **Figure 4**.

The HPU is located in Basement 2 (B2) level, 5 meters below the Ground level, and 45m far

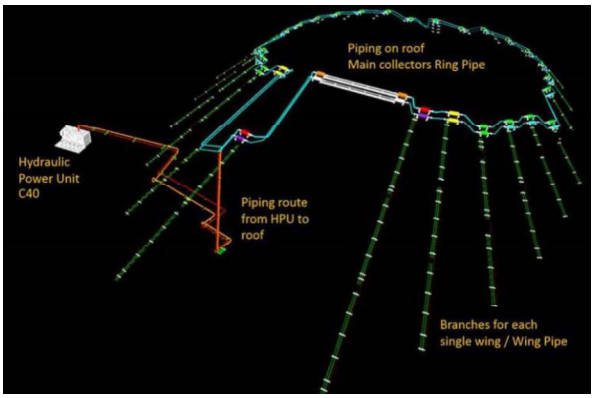

Figure 4: Pictorial view of the piping routed through the pavilion.

from the point where pipes can raise to the roof and approx. 100m from the farthest wing actuator: the design goal is the minimization of pressure losses along the distributions, in order to maintain a good system efficiency. This requirement, in conjunction with the design and test pressure set to 1.5 times the working pressure, leads to have a 5" size main pipe for the high-pressure line to the roof and an 8" size low pressure pipe for the fluid flow return from the roof to the power unit.

These two pipes are routed inside the pavilion B2 level to the designed *Riser* chimney, crossing parking, rooms, walls. This represents a real challenge considering that the weight is as high as 50 kg/m for bare steel without fluid inside for the 5" pressure line. Special supports, dedicated for each area, have been designed, taking into consideration the specific routing for both pressure and return line inside the pavilion area. Each support sustains more than half of a metric ton in such cases.

The vertical part of the pipes reaching the roof, called *Riser*, is a 15m long line ending at the interface between the concrete part of the pavilion and the steel roof. In this area the main design requirement is related to the ability to allow different deformation coefficients between the steel roof and the concrete part of the building. In fact, the steel roof is supported by the concrete structure in such a way, that it is free to move (breath) when contracting or expanding under thermal changes, in order to minimize the loads transferred from the roof into the concrete base.

On the roof, two pipes are formed in loop, passing through the steel roof ribs. These pipes, called *Ring Pipes,* ensure fluid distribution to each wing. Their size ranges between 4" and 3" for the pressure line and between 6" and 4" for the return line pipe. The diameter is at maximum near to the Riser and is reduced towards the ring termination. The ring topology has been chosen in order to let the fluid take the easiest, therefore less dissipative, way to reach the actuators according to each actuation phase. The ring is made with spool pieces connected by means of flanges, forming a segmented loop with many curves that allow deformation induced by thermal loads. The overall length of each loop is approx. 550m for the pressure pipe loop and 590m for the return pipe.

Flexible hoses have been used to connect *Riser* and Ring Piping. A system based on flexible seals and gutters is used for guaranteeing waterproofing of the roof where flexible hoses are installed.

Particular attention has been devoted to the design of the pipe supports. In fact, the pipe network has to be able to expand due to thermal effects induced by the oil temperature. Moreover, as the roof steel structure can be deformed by thermal effects and wind loads, the opposite condition has to be considered, allowing a roof deformation without impacting on the pipe integrity. Special supports have been designed for this purpose. Pipes are allowed to slide on them, being able to compensate thermal deformations. The fixation points have been designed allowing all degree of freedoms required to accommodate different thermal expansion coefficients. On the roof, the whole ring pipe is "floating" on these supports, allowing any deformation of the roof structure, without impacting the pipes.

An additional issue is represented by system vibrations that could be amplified by the steel structure of the roof generating noise inside the pavilion. For this reason, elastic elements have been introduced in correspondence of any connection point between the hydraulic system and the supporting structure. The complete piping network is sustained by adequate rubber pads.

Each wing is equipped with one to three actuators, according to the wing length, that needs to be fed with high pressure hydraulic fluid. For each wing smaller pipes are sufficient to provide the required flow. One high-pressure line and one return line run along the steel wing rib passing through valves manifolds used for feeding the system: these are called *Wing Pipes*. In order to reduce weight and volume and pipes

waste, pipe dimensions are different according the amount of flow they have to manage.

Connection between the ring and wing pipes are made with flex hoses in order to leave the ring pipes free to move and expand radially independently with respect to *Wing Pipes'* radial expansion.

2.3. Hydraulic Actuators and Motion Control

The movement of each hydraulic actuator is indipendently controlled by one dedicated proportional control valve. Additional valves are provided to manage lock-in position, emergency closing and direction of movement. Valves are installed on a block located on the back of each actuator, thus reducing the distance and increasing the control response time. Relief and lock valves are installed directly on the cylinder for safety purposes.

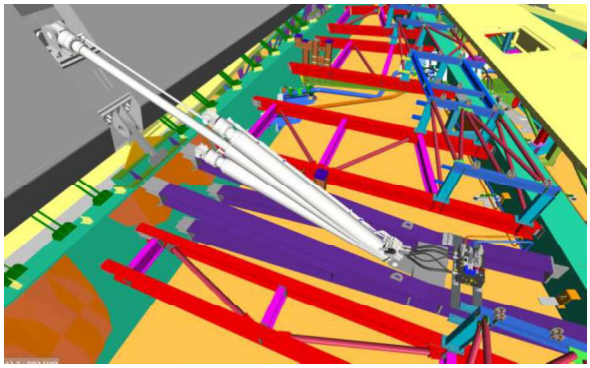

Figure 5: Valve Stand connected with hydraulic actuator.

The motion control solution has been designed in accordance to the specific hydraulic architecture and components. We have followed our standard philosophy in controlling the speed of a hydraulic axis piloting a compensated proportional flow valve and using the signal of a position transducer as feedback.

Two different hardware solutions have been adopted for controlling wings with single and multiple axes.

The system is modular. Each axis has a dedicated motion control card (CAC). In case of a multi-axis wing one additional control card acts as synchronism supervisor (SSC). All cards communicate internally via a dedicated CAN bus. The connection to the automation and control subsystem (AUT) is performed through a PROFINET interface.

Two different functions, discussed hereafter, are implemented in the motion controller: wing and synchronism control.

Wing control

It executes the opening/closing command, operating the wing. The angular speed profile according to [1] is defined by the distance, travel, acceleration and deceleration times with the following equation:

$$\omega_{MAX} = \frac{\alpha_{Tot}}{T_{TOT} - \frac{1}{2}(T_a + T_d)} \quad (1)$$

T_a and T_d have been chosen according to the hydraulic circuit characteristics and power management requirements.

The standard profile consists of a full-stroke opening/closing movement to be performed in 180s +/-2s. Fast closing with max. speed shall be allowed in 120s in case of critical weather conditions. Although it does not represent a nominal working condition, a profile generator allows a recovery movement starting from an intermediate position.

Due to the specific characteristics of the project and the difficulty in predicting the dynamic behaviour of the wing, a special open-loop algorithm has been implemented for controlling the angular speed of the wing using the stroke information of the cylinder as feedback.

The kinematic law of each actuator is defined by equation (2), that has a set of parameters that depend on the geometry and the position of the wing on the roof. Consequently, each cylinder has a unique parameters' set, that is stored in the firmware.

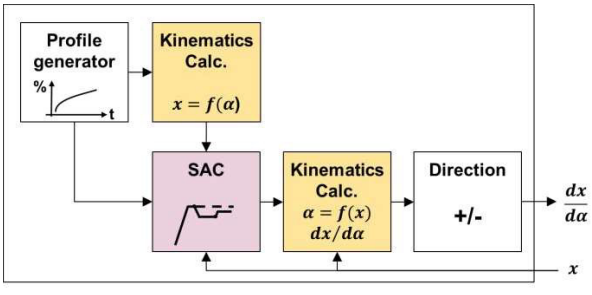

Figure 6: Block diagram of the motion control card algorithm for single axes wings.

$$\alpha[°] = cos^{-1}\left(\frac{R^2 + B^2 - (A_{CYL} + x[mm])^2}{2BR}\right) \times \frac{180}{\pi} \quad (2)$$

Based on the actual position x, the kinematic law is used to calculate the angle, and through the inverted relationship (3), to generate a linear position profile starting from the angular profile required by the travel time-direction relationship.

$$x[\text{mm}] = \sqrt{R^2 + B^2 - 2BR\cos\alpha} - A_{CYL} \quad (3)$$

A derivative function of the kinematic law is used to calculate the output to the proportional flow valve from the angular speed and to scale the control deviation due to the synchronism error in case of a multi-axis subsystem.

$$\frac{dx}{d\alpha} = \frac{2RB\sin\alpha}{2(x+A_{CYL})} \quad (4)$$

Due to the open loop control solution adopted, the tracking quality of the cinematic profile is strictly linked to the behaviour of the proportional flow valve, which has been designed "ad hoc" for this project. In order to compensate for deviations from the theoretical behaviour induced by external influences and tolerances in mechanical and hydraulic components, a Speed Adaptive Control (SAC) algorithm has been used. SAC is a modified version of the MR-Controls concept according to [2], with three main differences:

- SAC doesn't act at the same frequency of the control loop (i.e. 1 kHz), but in a defined number of checkpoints as a supervisor of the followed profile.
- SAC forces a direct correction to the speed at each checkpoint and compensates the cumulated positioning error in the remaining part of the stroke.
- Checkpoints are equally spaced in the angular range.

b. Synchronism control

Synchronization is required for wings with two or three axes. In this case the management of the Open Loop Profile and SAC are moved to SSC. This is required as the cinematics of the axes belonging to the same wing are different so that a normalized profile is required.

A closed-loop PI control (fc = 1kHz) based on a Master-Slave concept is implemented in CAC, using the synchronization set point passed by the SSC and it's active only for slave axes. The aim is to minimize the synchronism error under the maximum acceptable limit of +/-10mm around the normalized linear position.

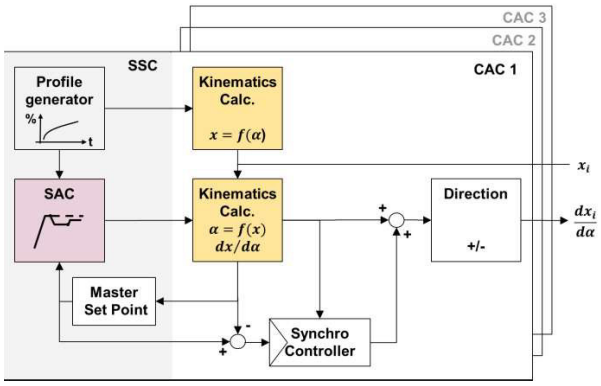

Figure 7: Block diagram of the motion control card algorithm for multiple axes wings.

The main advantages of this choice are:

- With a Master-Slave concept disturbances and oscillations on a slave axis do not influence the whole controller.
- The Master is controlled in open-loop avoiding the complexity arising from the low natural frequency of the system and granting the independence of the tuning of the synchro controller from the wing control.
- SSC, being the fastest observer of the synchronism, is also in charge for the execution of any immediate stop of the wing movement, in case that the synchronization error exceeds an acceptable threshold limit.

2.4. The Control and Automation Subsystem

The AUT subsystem manages the control of all RWOS parts and includes the following main items:

- One HPU Power Supply Cabinet including main PLC (HPU0-Q001)
- Two Wing Power Distribution Cabinets incl. remote PLCs for remote Wing Automation (HPU0-Q003 and -Q004)
- Four Wing Power Supply Cabinets delivering +24V power supply for all actuator subsystems (OCL0-Q001 through -Q004)
- Ten Wing Automation Cabinets including the control electronics for the actuator control and synchronization (OCL0-Q101 through -Q110).
- Several IP67 compliant remote I/O modules

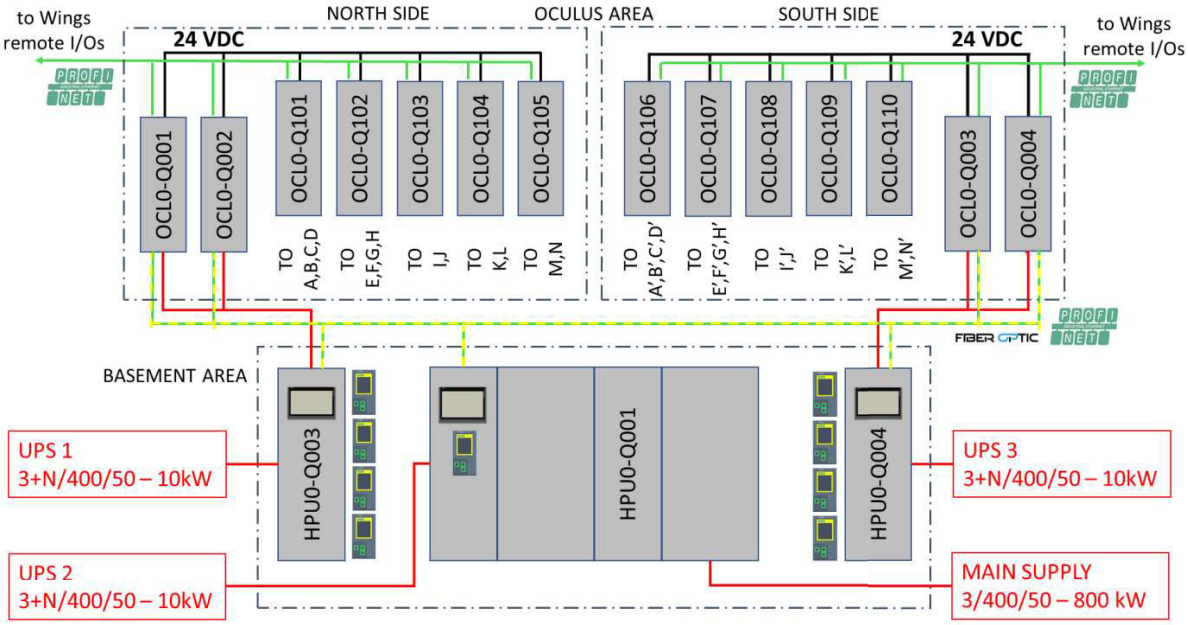

Figure 8: Block diagram of the RWOS AUT architecture including the network communication.

- Temperature sensors, pressure and stroke transducers
- Interconnecting harness including power cables, fiber optic lines, signal lines, sockets and sensors.

All PLCs are physically located in B2. Wing Power Supply and Automation Cabinets are located in the upper part of the roof, called Oculus. No direct roof access is required, since parametrization of any device can be performed remotely, thus simplifying the maintenance.

The roof opening and closing functionality is available from a central Building Management System (BMS) located in a dedicated area of the building through a dedicated network connection to the main PLC. A scheduler allows the execution of automated sequences based on daily or weekly wing actuation plans. Actuation sequences are limited to the maximum allowed cycles per day and maximum delay time between two consecutive cycles, in order not to overheat the hydraulic fluid.

The top-level block diagram of the RWOS is shown in **Figure 8**. The primary power to the HPU inverters and motors is delivered through the main cabinet HPU0-Q001 that is connected

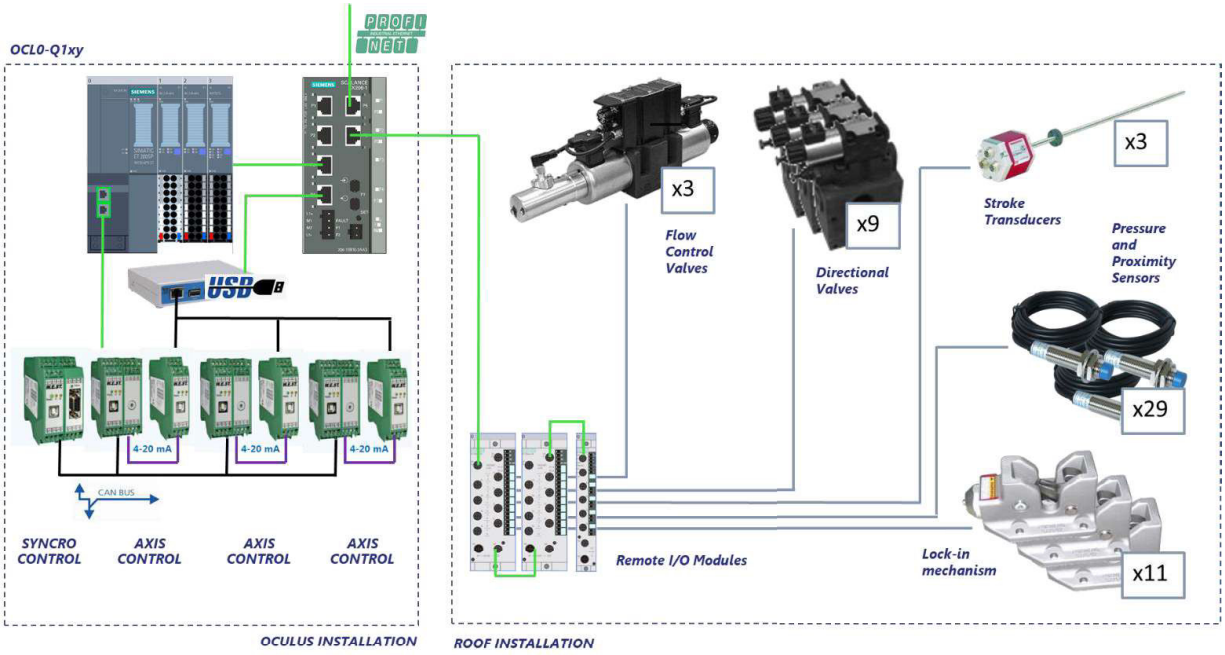

Figure 9: Subsystems connected to one multi-axes wing.

directly to the main transformer and is capable to provide up to 935kW of power.

All control subsystems of all electric panels including the main PLCs are supplied by three UPS subsystems, which allow 10 minutes of operation also in case of main power loss, thus ensuring the possibility to drive the RWOS in a secure condition before switch-off.

For each actuator the wing control electronics has to manage the following subsystems:

- Directional and proportional flow control valves for cylinder actuation
- Pressure transducers
- Stroke transducers
- Temperature sensors

In addition to the above, each wing has a certain number of additional valves for controlling the lock-in mechanism of the wings and for maintenance purposes.

Remote input/output modules are used at each actuator position, complying with the high-temperature requirements applicable to the roof area and IP67 protection class. Each socket is connected to the PROFINET communication network and receives the +24V power supply from the power supply cabinets installed in the Oculus area, as shown in **Figure 9**.

3. EARLY-STAGE SYSTEM VERIFICATION

3.1. Overall Approach

The main verification challenge is related to the system dimensions and to the difficulty of performing representative tests before final testing and commissioning at site. We have overcome this limitation following a V-model verification approach combining system modelling, simulations and tests at subsystem level. In particular, three levels of verification have been addressed, involving:

- The firmware of both CAC and SSC;
- The wing control subsystem including hydraulics, electronics and software;
- The system behavior, that depends from the hydraulics architecture, the operation of the wings and disturbances generated by both internal and external factors (i.e. pressure fluctuations, wind effects, etc.).

The testing activity has been aimed to anticipate the behavior of the components involved in the system and to identify the risks during the development phase prior to the testing at site. In the following paragraphs we provide an overview of each verification steps, starting from the system modelling, which represents the base of our verification strategy.

3.2. System Modelling and Simulations

System simulations have the objective of identifying critical working conditions during test, commissioning or operational phases. The criterion is the verification of the available system design margin. Two main aspects have been analyzed:

- System pressure losses throughout the various operating conditions, that depend from the power demanded by the actuators during the movement. They answer to the basic question if the cylinders are able to move in any possible load condition.
- Pressure reserve available under worst case operating conditions.

Different simulation models have been developed for this purpose.

Evaluation of pressure losses

The first model includes HPU, pressure relief valves (PRV) used for setting the system pressure and piping network. The pump model is signal-based. The hydro-mechanical and volumetric efficiencies are stored in a map. Both are dependent from the applied system pressure and engine speed, according to . This allows the calculation of the effective torque of the motor shaft and the loss of the volume flow to along its characteristic curve, from the start up to the operating point. The parameterisation and validation are executed with data sheets and pump characterization measurements. The model does not consider the dynamic behaviour and pulsation of the pump, as well as the starting behaviour of the electrical motors.

The manifold includes different valves and filters that have been described exclusively by their flow characteristics. A functional mapping is not necessary, as these are normally only actuated when the system is not moving. The PRV model is based on the functional description of the valve based on pressure-time profiles, dynamic behaviour and volume-flow characteristics.

Design data including lengths, diameters and height differences have been used for the pipe

system model, which is composed by individual pipe elements. Every element considers:

- hydraulic capacity and inductance

$$L_h = \rho \cdot \frac{l}{h} \quad (5)$$

$$p_{acceleration} = L_h \cdot \frac{dQ}{dt} \quad (6)$$

$$C_h = \frac{A}{\rho \cdot g} \quad (7)$$

$$\dot{p} = \frac{1}{C_h}(Q_{in} - Q_{out}) \quad (8)$$

- hydrostatic losses

$$p_{hydrostat} = g \cdot \rho \cdot h \quad (9)$$

- hydrodynamic losses

$$p_{hydrodym} = \zeta \cdot \frac{\rho}{2} \cdot v^2 \quad (10)$$

$$\zeta = \zeta_{pipe} + n_{bend} \cdot \zeta_{bend} + \zeta_{res} \quad (11)$$

- pipe friction according to Haaland

$$\zeta_{pipe} = \lambda(Re) \cdot \frac{l}{d_i} \quad (12)$$

- flow resistance

$$\zeta_{res} = \frac{K_{Lam}}{Re} + \zeta_T \quad (13)$$

Pipe wall expansion effects and fixation interfaces to the building structure were neglected as their real effect on the system was unknown at the time.

Pipe model validation has been limited to a first-order validation based on literature [3], due to the non-availability of measurements and the large scale of the system.

All cylinders have been mapped with their required volume flow through 46 take-over points directly connected to the main piping circuit.

Every sub-model including the related physical behavior has been verified individually before final model assembly.

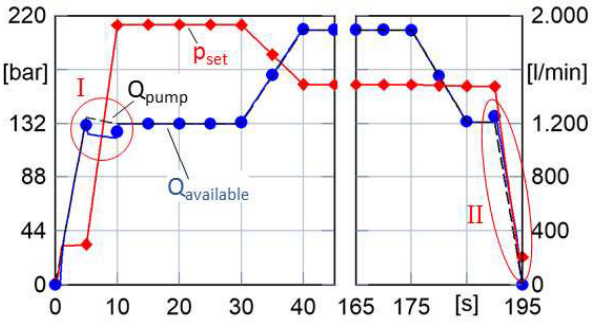

Figure 10: Influence of the hydraulic capacity - pressure build-up and down phase

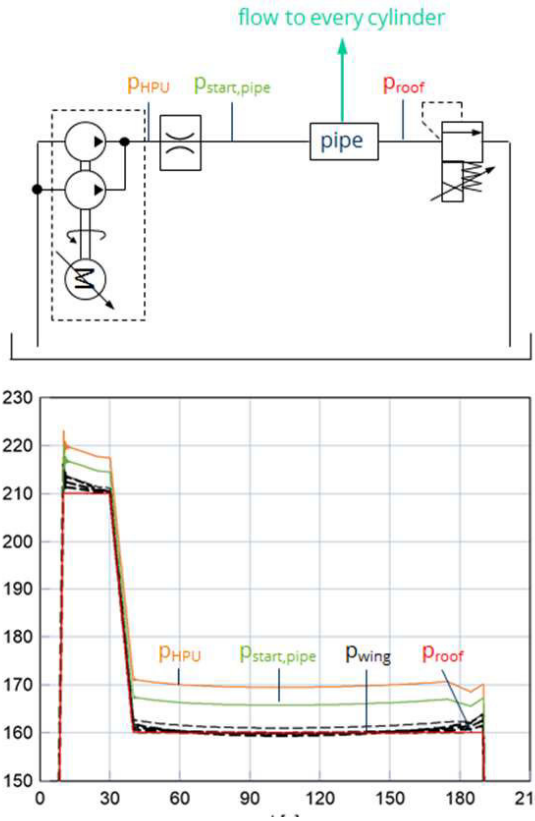

Figure 11: Pressure losses simulation for opening cycle (180 sec, PRV on the roof).

Figure 10 shows an example of the intermediate verification: The influence of the hydraulic capacity on the pressure build-up (I) and drop-down (II) phases for the opening cycle without cylinder flow and other losses is illustrated. In area I, the difference between pump flow and available flow over the PRV is the necessary volume flow for the system pressure build-up. Area II shows an additional volume flow in the pressure drop-down phase.

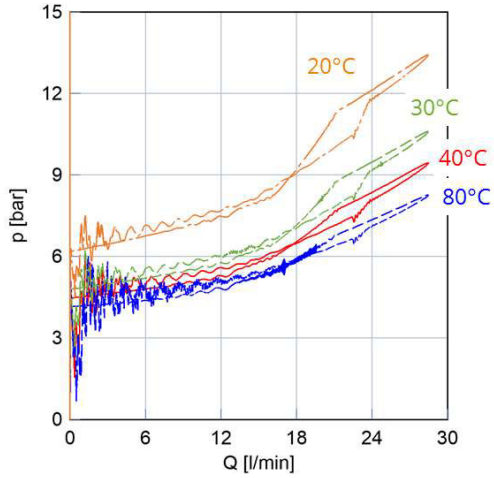

Figure 12: Pressure losses vs. volume flow on cylinder A2 at different temperatures (HLP 46).

Figure 11 presents the results of the pressure loss analysis for the 180 sec opening cycle. The pressure at different locations is shown for HLP46 oil at 40°C. Losses are approximately 10 bar, as expected.

Four temperatures and two oil types have been analyzed, as shown in **Figure 12**, where pressure losses at the cylinder connection joint are shown as a function of the volume flow. Worst-case pressure losses are 13bar at 20°C oil temperature. 15bar have been considered through all simulation work, in order to compensate for model uncertainties and measuring errors from the preliminary investigations.

Evaluation of the pressure reserve

The evaluation of the system pressure reserve requires the modelling of the cylinder hydraulic control, that includes the flow control valve (FCV), as well as additional components. The system behaviour is defined by the FCV characteristics. Depending on the cylinder size, two valve types with nominal volume flows of 60 l/min or 110 l/min respectively have been used. All other components have been modelled exclusively by their flow characteristics.

The FCV includes proportional valve spool, pressure compensator, and pilot valve. The volume flow is kept constant with changing load conditions for a constant set current. This is achieved through the pressure compensator, that ensures a constant pressure drop across a throttle, according to the following throttle equation:

$$Q_{Valve} = \alpha \cdot \sqrt{\frac{2}{\rho}} \cdot A_{Throttel} \sqrt{\Delta p} \qquad (14)$$

The FCV has typically non-ideal behaviour, that includes current and pressure dependent flow characteristics and hysteresis. The valve control range begins at a pressure drop of eight bar. The model includes the following components:

- a characteristic valve map;
- a set current dependent hysteresis;
- the valve behavior outside the pressure control range.

Signal-based mapping has been used for the determination of the characteristic FCV map. For this purpose, measurements of the valve recorded in four different set-up configurations have been used and analysed, in order to derive the basic characteristics of the components involved. **Figure 13** shows the valve measurement setup. During the test a pump is providing a constant volume flow. Two different PRV can set a nearly constant pressure difference across the flow control valve. The following test scenarios have been used:

1. ramp-shaped current build-up without counter pressure
2. ramp-shaped current build-up with constant counter pressure at 180 bar
3. ramp-shaped counter pressure build-up with constant opening current at 1900 mA
4. ramp-shaped counter pressure build-up with constant opening current at 1260 mA

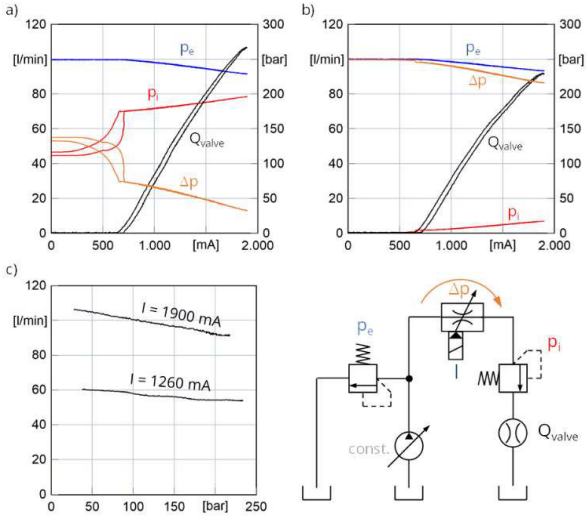

Figure 13: Sketch of the measurement test bench and results – a) with counter pressure; b) without counter pressure; c) two measurement with constant current by changing pressure difference.

The characteristic valve map is derived by fitting the known measured points with polynomial functions using a least squares approximation. The maps generated so far are further reduced to final characteristic maps with significantly less points through a second least squares approximation. The result are characteristic maps that are transferred into the model. Out of the valve pressure control range – i.e. between 0 to 8 bar – the valve behaviour is approximated with an ideal throttle equation, according to (14).

The theoretical derived pressure dependence is evident in the characteristic diagram. Considering a constant set current of 1900 mA, approx. 21 l/min total flowrate variation are generated at the maximum pressure difference. Furthermore, it can be seen that there is no clear linearity between volume flow and control current. Both aspects have to be taken into account when reflecting the control algorithm.

Based on the analysis of the measurement data, the following model components have been generated with an acceptable level of accuracy (**Figure 14).**

- Characteristic valve map

  $Q_{map} = f(\Delta p, I_{solenoid})$

- Hysteresis dependent on set current change

  $Q_{hyst} = f(I_{solenoid}, dI_{solenoid})$

- Ideal throttle behavior beyond control range

  $Q_{ctrl} = f(\Delta p)$

Pressure dependent hysteresis has been neglected.

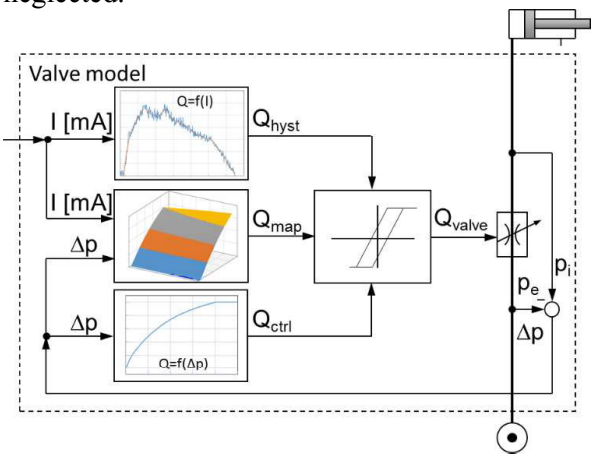

Figure 14: FCV Model.

The model considers the time response of the FCV. Two approaches have been investigated. In the first option, the reaction time of the pressure compensator to changing pressure conditions can be simulated by a delay in the pressure difference signal. In the second approach the signal of the solenoid control current is delayed. Considering the dynamic behaviour of the valve that depends mainly on inertia and friction, a time-dependent solenoid current has been preferred.

The evaluation of the pressure reserve has been carried out with the above model. We have selected the most critical cylinders in terms of loads generated by the wing mass and external forces in worst-case wind conditions. The highest force on each wing angle position under all wings was used to create a synthetic force load profile for the simulation.

Both the opening and closing sequence have been separately investigated. Reaction forces on the cylinder and the pressure on the cylinder valve block have been considered as model boundaries. The applied system pressure has been reduced by 15 bar in order to account for pressure losses. A simplified version of the cylinder control algorithm has been used for this purpose.

First results evidenced the necessity for modifying the system pressure profile extending the duration of the high-pressure condition at the beginning of the opening cycle, in order to overcome the high loads acting on the actuators. Also, during the closing process pressures were insufficient in some cases.

New profiles have been generated increasing the system pressure from 140 to 160 bar showing that sufficient design margin is present during all operating conditions. An example is given in **Figure 15**, where the results for the most heavily loaded cylinder in the closing phase are shown for the above-mentioned pressure conditions. The pressure difference between piston and return line shall exceed the minimum difference required by the pressure compensator of the FCV, that is 8 bar, in all operating conditions providing an adequate margin. Increasing the system pressure ensures an increase of this value from 0.5 bar to 25.5 bar.

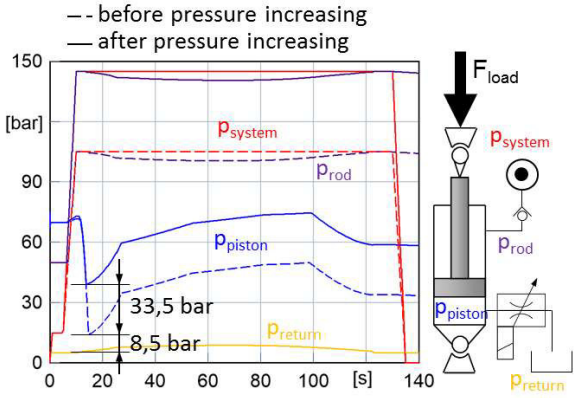

Figure 15: Pressure difference across the FCV throughout the closing cycle.

3.3. Verification of the actuator control algorithms

Hardware-in-the-Loop Test Bench

The tests performed on the software code to verify the behaviour of the control are usually not sufficient to identify all critical working conditions, since with a simple software testing environment it is not possible to reproduce the changing environmental conditions in which the algorithms are supposed to work. For this purpose, a Hardware-in-the-Loop (HiL) system

has been designed and implemented. Hardware-in-the-Loop (HiL) simulation is a common technique used for system-level testing of embedded systems. The HiL test bench contains a virtual simulation environment that includes the cylinder subsystem and different hardware components, as shown in **Figure 16**.

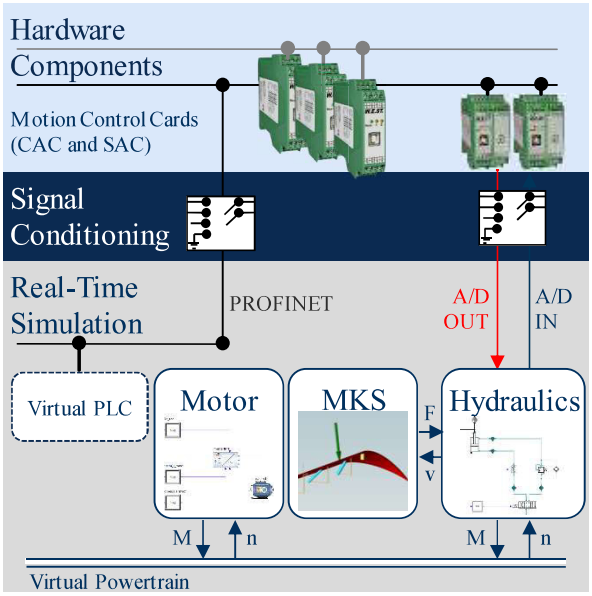

Figure 16: Hardware-in-the-Loop test bench

The test bench can simulate virtual movements of the wings, which are controlled by the motion control cards (CAC and SAC) incl. the corresponding hydraulic valves. Signal conditioning is managed by a dedicated Field Programmable Gate Array (FPGA) and communication occurs through PROFINET fieldbus. The main objective has been the test of the motion control algorithms, answering to the following questions:

1. Has the general functionality been achieved? Have all software bugs been identified?
2. Are the requirements fulfilled? In particular, can the opening/closing time requirements be achieved with the given maximum position error under all circumstances?
3. How sensitive is the influence of different controller parameter on the performance?

Two groups of test cases have been generated for this purpose, in order to study the performance of synchronized actuator movement under safety critical conditions and for specific failure simulations.

Three main results have been obtained by Hardware-in-the-Loop simulation:

- The specific designed Speed Adaptive Control algorithm is able to control the position error within the specified limit of +/- 10mm during both opening and closing movements for all wings under worst-case load conditions. The opening/closing time requirements (180s/120s +/- 2s) can be met for all test cases. The compliance in terms of time tolerances is a precondition in order to ensure the synchronous movement of all wings on the roof.
- The SSC controller for the movement of wings with more than one axis complies the demanded tolerances for angular deviation during all test cases. The compliance of these tolerances is absolutely necessary for guarantying low bending moments of the wings and therefore a damage-free wing movement.
- The influence of component specific tolerances, as for instance stroke-sensor offset fluctuations, are not affecting the system performance. The wing opening and closing movement can be guaranteed under all conditions.

Figure 17 shows the results for the opening cycle on multi-axes wing L. The three curves represent the angular cylinder deviations α for the three axes.

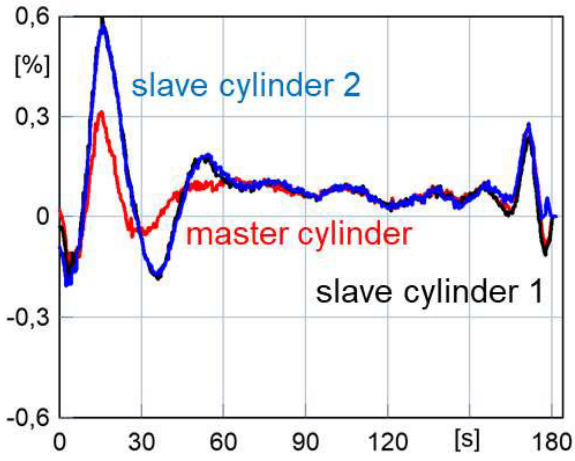

Figure 17: Position error [%] - Testcase 5b), opening 180s cycle with wing L2 as master cylinder und dead-load condition and offset

After the initial 20s acceleration ramp at the beginning of the movement, the error on all three cylinders is decreasing to zero. This condition is maintained throughout the linear movement until the deceleration ramp is started. The speed adaption algorithm is compensating the stroke error correctly, by adapting the speed of the movement. Slave cylinders are behaving in

agreement with the master cylinder (one), showing that the PI controller responsible for axes synchronization is working properly. Throughout the movement all specified tolerances are within the requirements.

Wing Test Bench

The wing test bench is a versatile hardware replica of a wing subsystem, built and stored at DMS premises. Although downscaled to limit occupied space and energy consumption, it accurately replicates the properties of both a single and a multiple axes wing installed on the pavilion.

The wing test bench is composed by the following equipment:

- 3 hydraulics cylinders (stroke 1000mm, bore 50mm, rod 28mm) including SSI linear transducers, the related control axes boards and valve blocks.
- Hydraulic Power Unit (HPU) working at 120bar and fixed flow rate.
- Control PLC, acting as the wing controller;
- Ancillary equipment (sensors, remote I/O-modules, HMI).

The main objectives of the replicated wing system are:

- Validation of the firmware implementation in the motion control boards;
- Debugging and early-validation of the automation software.

In order to thoroughly test the motion algorithms, the hydraulic circuit is equipped with additional proportional pressure valves that are used to inject external disturbances to simulate wind loads and test the algorithms robustness.

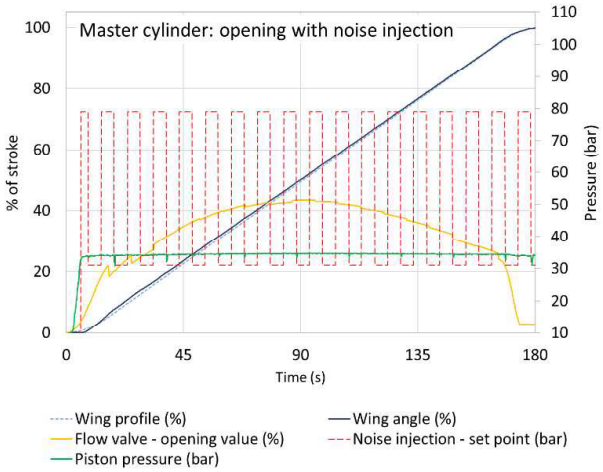

Figure 18: Opening movement with noise injection. Master cylinder.

Figure 18 and **Figure 19** show the results for master and slave axes for an opening movement performed in 180s, where the influence of external disturbances (e.g. wind forces) has been simulated by the injection of a noise pressure square wave.

As in Master-Slave controlled mode, the synchronism control loop that acts on each Slave is not affected by the behavior of other slave axes, a simplified sub-system with 2 axes only has been here represented. The master has been controlled in open loop with speed adaption acting approx. each 9s. Only low-frequency noise effects have been considered. Slave axes have been disturbed with a square waveform performing a frequency sweep (from 0.2 up to 5Hz).

The results confirm that the overall opening time is not affected by the influence of external forces, although the square wave profile creates alternating pushing and pulling forces. The robustness of the synchronization algorithm is demonstrated by the synchronization error on the slave axes, that is well below the max. acceptable threshold of +/-10mm. It has to be considered, that noise injections for master and slave were not in phase.

This can be observed in the slave behavior, where a “Delta noise injection” representing the normalized difference between Master and Slave noise injections is shown. The relationship between the proportional valve correction and the noise applied on both axes can be appreciated.

Overall Results

Simulations, HiL and WTB have generated results that confirm the feasibility and reliability

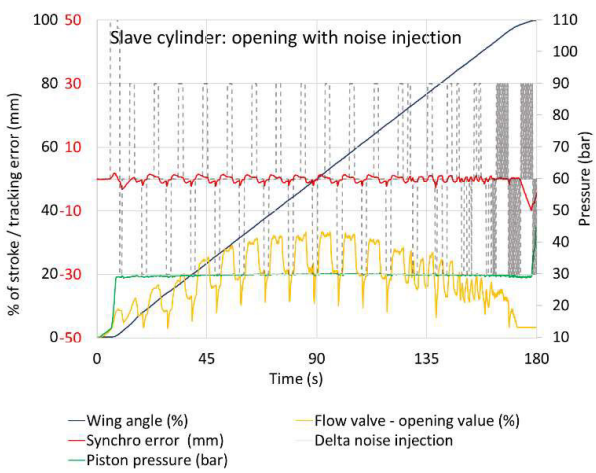

Figure 19: Opening movement with noise injection. Slave cylinder.

of the technical solution proposed, demonstrating in particular the robustness of the synchronism algorithm, but highlighting critical aspects, too.

The necessity of a non-linear characteristic curve for the proportional flow valves, the choice of the proper cylinder as a master in a multi-axis system, the modified ramp-times and pressure levels in the flow-pressure timeline for opening/closing movements are examples of corrective actions implemented during the development that will reduce effort and unexpected events during commissioning.

On the other side, some simplifications on the model and not fully validated behaviors in the simulations will require a deep analysis of the real system at site. Particular care shall be devoted to the choice of wing-level cinematics parameters that shall consider the actual manufacturing tolerances, as well the fine tuning of the synchronism controller.

4. ERECTION & COMMISSIONING

4.1. Activities at Site

Installation of the equipment on site has been running since January 2019. One major difficulty we encountered is related to the coordination with the other activities involving the building. Usually, complex equipment is installed after the completion of civil works. In our case this has not been possible, due to the very aggressive time schedule, the complexity of the building and the technical difficulties encountered in the coordination among different Subcontractors. At the time where this paper is being prepared, the complete piping system only has been fully installed and commissioned, including 10 single axes wings and the first four three-axes wing. Electric installations are still on-going preventing the operation of the wings with the main HPU. Therefore, additional auxiliary equipment has been designed and build in order to allow pre-commissioning and anticipate critical tests.

4.2. Single-axis wings

Ten single axes wings have already been installed and fully tested. The pressure flow for the movement is provided by an auxiliary HPU that is connected to the system piping through by-pass flanges in Basement 2. For the movement the wing angle has been monitored through dedicated transducers and the values compared with the stroke transducer position information of the cylinder. The calculated wing cinematic parameters based on as-built conditions are very close to the original as-designed parameter, although installation tolerances are in general significantly higher than as-designed ones.

The wing behavior during one opening cycle is shown in **Figure 20**.

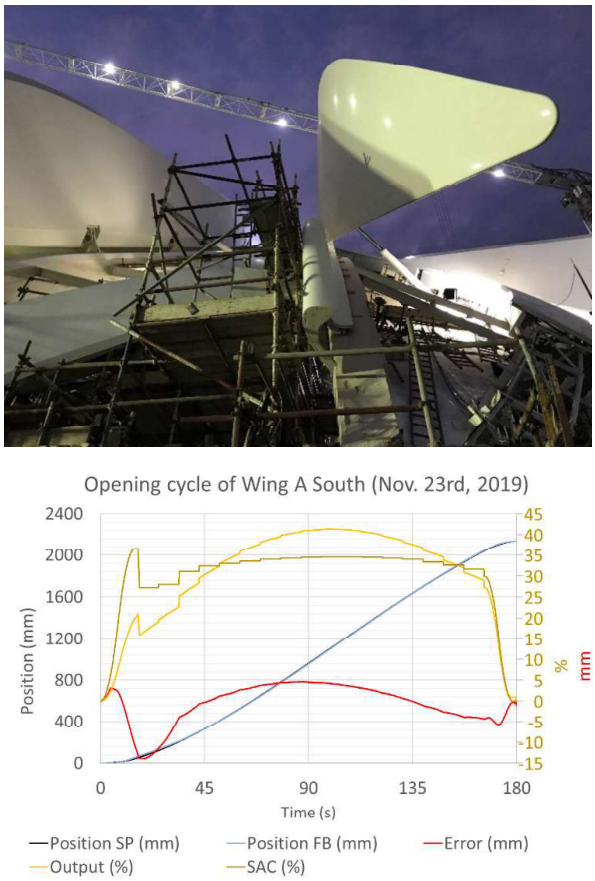

Figure 20: Pre-commissioning results on wing A South.

The blue curve represents the stroke of the opening movement. The total travel time is 180,3 seconds, within the specified limit of 180s +/- 2s. The function of the SAC can be observed on the yellow curve. After the first two checkpoints stroke errors are compensated adjusting the speed profile. This is confirmed by the stroke error that reaches its maximum at the first checkpoint, after which compensation occurs.

5. CONCLUSIONS

The Roof Wing Opening System for the UAE Pavilion at Expo 2020 has been presented, showing both the very special requirements related to this particular application and the boundary conditions of the project, that require a different approach compared to conventional

industrial applications. The early-stage verification approach based on the joint use of system simulations, tests at component and subsystem level, as well as pre-commissioning activities at site has been discussed. All results show the validity of our approach and represent a good base for the commissioning activities on the pavilion, that will run on a limited time-frame in spring 2020.

The authors would like to thank Mr. Ulrich and Mr. Winkes of W.E.ST. Elektronik GmbH, Ms. Hina Farooqi and the whole Calatrava International Team for the continuous support and fruitful discussions throughout the whole project. A special thanks to Arabtec Construction Team for its logistic support on site.

NOMENCLATURE

A	Area
A_{CYL}	Cylinder Length in the fully retracted position
AUT	Automation and Control Subsystem
B2	Basement 2
CAC	Single-Axis Control Card
DME	Duplomatic Middle East LLC
DMS	Duplomatic Motion Solutions S.p.A.
FCV	Flow Control Valve
FW	Firmware
HiL	Hardware-In-the-Loop
HMI	Human-Machine Interface
HPU	Hydraulic Power Unit
I/O	Input/Output
IFK	International Conference of Fluid Power
MR	Multi-Recursive
PLC	Programmable Logic Controller
PRV	Pressure Relief Valve
RWOS	Roof Wing Opening System
SAC	Speed Adaptive Control
SSC	Synchronism Supervisor Card
SW	Software
ω_{MAX}	Maximum Angular Speed
α_{Tot}	Angular Range
T_{Tot}	Total Time
T_a	Acceleration Time
T_d	Deceleration Time

REFERENCES

[1] Jack L Johnson - Designer's handbook for electro hydraulic servo and proportional systems

[2] Ulrich Walter (W.E.St.) - A multiplicative-recursive filter and linearization scheme

[3] I.E. Idel'chik, [*Handbook of hydraulic Resistance – Coefficients of Local Resistance and of Friction*, 1960, Moscow]